



Porosity–strength relation in calcium aluminate cement pastes

T. Matusinović*, J. Šipušić, N. Vrbos

Department of Inorganic Chemical Technology and Nonmetals, Faculty of Chemical Engineering and Technology, University of Zagreb, Marulićev trg 20, HR-10000 Zagreb, Croatia

Received 26 March 2002; accepted 2 June 2003

Abstract

The compressive strength and the volume porosity of calcium aluminate cement pastes have been studied in order to connect their relationship. The influence of mass fraction of lithium carbonate on compressive strength and porosity of calcium aluminate cement (CAC) has been investigated at different water–cement (w/c) ratios. The functions proposed in the literature for different technical materials were tested on obtained strength and porosity data. Those functions have been a base for further development of more general functional dependence of strength and porosity for cement materials. Thus, we propose the following equation to relate the strength and porosity for CAC pastes:

$$\sigma = \sigma_{P_0} \left(1 - \frac{P}{P_0} \right)^2$$

© 2003 Elsevier Ltd. All rights reserved.

Keywords: Calcium aluminate cement; Lithium compounds; Compressive strength; Modeling; Porosity

1. Introduction

Although the setting and hardening of calcium aluminate cement (CAC) represents a process of commercial and industrial importance, the chemical processes involved during the hydration are not yet well understood. The set of CAC may be considerably influenced by addition of small quantities of alkali metal salts [1–7]. Along with rapid setting, lithium salts cause the strength development at very early ages [8]. Hydration of CAC proceeds through initial dissolution of CAC and subsequent precipitation of calcium aluminate hydrates, which is accompanied by increase in strength and decrease in porosity [4,9,10]. Physical properties of materials, compressive strength, and volume porosity have been studied in order to connect their relationship.

Balshin [11] suggested the following equation for porous metal ceramic (Eq. (1)):

$$\sigma = \sigma_{P_0} (1 - P)^k \quad (1)$$

* Corresponding author. Tel.: +385-1-4597-218; fax: +385-1-4597-250.

E-mail address: tmatusin@pierre.fkit.hr (T. Matusinović).

σ —strength; σ_{P_0} —strength at zero porosity (constant value for a given material); P —porosity; k —empirical constant.

Ryshkewitch [12] suggested the following equation for porous sintered alumina and zirconia (Eq. (2)):

$$\sigma = \sigma_{P_0} e^{-kP} \quad (2)$$

σ_{P_0} —strength at zero porosity (constant value for a given material); k —empirical constant.

Schiller [13] suggested the following equation for gypsum pastes (Eq. (3)):

$$\sigma = k \ln \left(\frac{P_0}{P} \right) \quad (3)$$

k —empirical constant; P_0 —porosity at zero strength.

Hasselmann [14] suggested the equation of a linear relationship between strength and porosity for different refractory materials (Eq. (4)):

$$\sigma = \sigma_{P_0} - kP \quad (4)$$

σ_{P_0} —strength at zero porosity; k —empirical constant.

Table 1

Experimental results of compressive strength and porosity measurement for the CAC materials at $w/c = 0.20$, prepared with addition of Li_2CO_3

t (h)	σ (MPa)	TW (%)	BW (%)	ρ_s (g cm ⁻³)	P (%)
$w(Li_2CO_3) = 0\%$					
1	—	16.32	1.05	3.34	37.87
2	—	16.50	1.18	3.33	37.93
3	0.9	16.70	1.84	3.33	37.27
4	1.3	16.73	2.55	3.28	35.84
5	8.6	17.01	5.53	3.21	30.75
6	14.1	18.16	11.56	3.12	20.10
7	25.3	18.18	14.16	3.02	12.92
8	32.5	18.22	15.01	2.98	10.47
9	43.8	18.34	15.08	2.81	10.09
24	57.5	18.40	16.04	2.80	7.49
72	61.5	18.43	16.33	2.64	6.36
168	64.5	18.93	17.67	2.57	3.84
$w(Li_2CO_3) = 0.001\%$					
1	—	17.13	2.75	3.05	34.61
2	0.3	17.37	2.80	2.85	33.45
3	0.6	17.53	5.79	2.78	28.35
4	2.5	18.38	8.82	2.73	24.23
5	11.0	18.99	12.20	2.69	18.40
6	28.8	19.27	13.69	2.54	14.94
24	40.0	20.20	15.50	2.39	12.34
72	47.9	20.31	16.66	2.41	9.94
168	56.6	20.35	17.69	2.39	7.39
$w(Li_2CO_3) = 0.003\%$					
1	0.3	17.08	1.08	3.07	37.20
2	0.4	17.38	2.83	3.05	34.94
3	1.9	18.87	3.99	2.88	34.56
4	19.4	18.81	11.62	2.74	19.53
5	35.3	18.90	13.67	2.56	14.17
6	46.8	19.24	14.19	2.50	13.52
24	59.9	19.26	15.42	2.46	10.47
72	66.8	20.65	17.28	2.46	9.46
168	73.6	20.68	18.36	2.45	6.69
$w(Li_2CO_3) = 0.005\%$					
1	0.9	16.07	2.00	3.31	35.69
2	2.8	17.48	3.12	2.98	34.15
3	11.8	18.30	9.97	2.85	22.52
4	22.9	18.34	13.02	2.82	15.52
5	50.1	18.43	13.86	2.78	13.48
6	68.7	18.63	15.12	2.67	10.33
24	72.1	18.71	15.81	2.62	8.55
72	74.5	18.80	16.51	2.50	6.59
168	76.1	19.09	17.50	2.48	4.65
$w(Li_2CO_3) = 0.007\%$					
1	1.3	17.43	4.00	2.96	32.50
2	4.8	17.73	4.55	2.84	31.27
3	14.8	18.45	9.90	2.63	21.61
4	25.3	19.16	12.94	2.58	16.56
5	46.4	19.27	14.65	2.55	12.73
6	62.4	19.33	15.65	2.52	10.31
24	72.1	19.97	17.01	2.39	8.12
72	74.5	20.14	17.77	2.43	6.73
168	76.1	20.55	18.59	2.41	5.61
$w(Li_2CO_3) = 0.010\%$					
1	1.6	15.92	2.32	3.20	34.11
2	12.0	17.69	8.60	2.92	24.38
3	26.0	18.38	12.60	2.74	16.25

Table 1 (continued)

t (h)	σ (MPa)	TW (%)	BW (%)	ρ_s (g cm ⁻³)	P (%)
$w(Li_2CO_3) = 0.010\%$					
4	33.9	18.40	13.71	2.68	13.35
5	42.5	18.60	14.24	2.63	12.35
6	45.8	18.56	14.83	2.59	10.60
24	64.8	19.61	16.58	2.57	8.83
72	72.2	19.69	17.34	2.49	6.79
168	74.6	19.99	17.74	2.47	6.49

Functions proposed in the literature [11–14] were tested on strength and porosity data obtained in this work, and the new function relating the strength and porosity for cement materials was proposed.

2. Methods

The CAC used was taken from a regular production of Istra Cement International, Pula, Croatia, part of Heidelberg Zement Group. The cement has the following composition (mass %): CaO, 40.2%; Al_2O_3 , 39.0%; Fe_2O_3 , 11.7%; FeO, 4.3%; and SiO_2 , 1.9%. The principal mineral phase is monocalcium aluminate, $CaAl_2O_4$ (CA), with $Ca_{12}Al_{14}O_{33}$ ($C_{12}A_7$), $Ca_6Al_2Fe_4O_{15}$ (C_6AF_2), and β - Ca_2SiO_4 (β -C₂S) as minor phases. Li_2CO_3 used was commercial Analar grade reagent.

2.1. Compressive strength measurement

Compressive tests were run on specimens according to ASTM C 349-77. The specimens ($40 \times 40 \times 160$ mm) were prepared according to ASTM C 109. Three specimens were tested for each age.

2.2. Total water (TW) and bounded water (BW) determination

TW is determined by weighting the CAC paste (obtained from the crushed specimens) before and after ignition at 1000 °C. Quantity of TW is expressed per 100 g of ignited material.

BW is determined on the separate portion of the same CAC paste taken after the compressive strength test. The paste is immediately mixed with acetone in order to stop the hydration and remove “free” or uncombined water. The quantity of chemically BW, which remains in the acetone-dried sample of CAC paste, is then determined in the same manner as the quantity of TW.

2.3. Density test

Average density of acetone-dried CAC paste, which includes the hydrates and the fraction of nonreacted cement, is determined according to the ASTM C 188-89. Porosity is defined as the fraction of the cement paste volume filled

Table 2

Experimental results of compressive strength and porosity measurement for the CAC materials at w/c=0.25, prepared with addition of Li_2CO_3

t (h)	σ (MPa)	TW (%)	BW (%)	ρ_s (g cm^{-3})	P (%)
$w(\text{Li}_2\text{CO}_3)=0\%$					
1	—	19.15	1.51	3.30	41.86
2	—	19.35	2.12	3.27	41.13
3	—	19.68	2.62	3.26	40.90
4	0.9	19.78	3.99	3.10	37.90
5	5.4	20.56	7.09	3.00	33.72
6	17.0	21.09	11.81	2.90	25.43
7	36.9	21.86	16.82	2.85	15.53
8	44.4	22.08	17.76	2.79	13.40
9	54.2	22.52	18.74	2.77	11.91
24	58.9	22.54	19.75	2.70	8.86
72	66.7	22.65	19.90	2.63	8.55
168	68.9	23.15	20.18	2.61	9.16

 $w(\text{Li}_2\text{CO}_3)=0.001\%$

1	—	20.05	2.45	3.05	40.17
2	—	20.32	2.89	3.01	39.70
3	0.8	21.89	8.82	2.74	31.44
4	12.1	22.09	13.62	2.65	22.37
5	31.0	22.17	15.85	2.56	17.21
6	48.9	22.38	16.81	2.48	15.11
24	68.8	23.11	19.97	2.39	8.89
72	71.1	23.21	20.83	2.39	6.90
168	74.0	23.57	21.37	2.36	6.36

 $w(\text{Li}_2\text{CO}_3)=0.003\%$

1	—	19.99	2.86	3.00	39.11
2	—	20.31	3.67	3.02	38.67
3	0.9	20.52	7.22	2.82	32.06
4	22.1	21.27	13.33	2.74	21.65
5	25.4	22.00	14.45	2.67	20.54
6	36.8	22.70	16.07	2.52	17.77
24	60.1	23.67	20.20	2.40	9.84
72	73.6	24.14	21.15	2.35	8.48
168	77.3	24.18	21.42	2.33	7.82

 $w(\text{Li}_2\text{CO}_3)=0.005\%$

1	0.3	21.34	2.24	3.12	43.10
2	2.7	21.42	7.26	3.04	35.39
3	28.9	21.45	13.50	2.75	21.77
4	32.1	21.50	15.75	2.61	16.05
5	38.8	21.85	16.20	2.57	15.67
6	40.4	21.85	16.34	2.54	15.19
24	43.3	22.05	16.96	2.58	14.42
72	47.4	22.80	18.18	2.50	13.01
168	48.0	23.81	19.43	2.50	12.57

 $w(\text{Li}_2\text{CO}_3)=0.007\%$

1	1.2	20.66	2.03	2.94	40.84
2	9.7	21.41	9.09	2.77	30.28
3	22.7	22.78	16.00	2.61	18.64
4	30.9	22.97	16.35	2.53	17.86
5	38.0	23.08	16.55	2.51	17.57
6	41.2	23.12	16.98	2.49	16.59
24	44.0	23.19	17.58	2.42	15.02
72	48.1	23.60	17.99	2.37	14.82
168	67.7	23.69	20.30	2.34	9.42

 $w(\text{Li}_2\text{CO}_3)=0.010\%$

1	4.3	20.04	2.65	3.05	39.88
2	9.4	20.85	8.00	2.89	31.94
3	31.2	20.90	13.57	2.76	20.37

Table 2 (continued)

t (h)	σ (MPa)	TW (%)	BW (%)	ρ_s (g cm^{-3})	P (%)
$w(\text{Li}_2\text{CO}_3)=0.010\%$					
4	40.3	20.93	15.78	2.60	14.48
5	45.8	20.94	16.15	2.53	13.29
6	50.0	21.33	16.83	2.53	12.64
24	58.7	21.95	18.63	2.55	9.79
72	71.0	21.86	18.58	2.46	9.36
168	76.9	21.95	19.07	2.37	8.04

with “free” water and is calculated according to the formula (Eq. (5)) [10]:

$$P = \frac{(TW - BW)/\rho_{\text{H}_2\text{O}}}{\frac{100 + BW}{\rho_s} + \frac{TW - BW}{\rho_{\text{H}_2\text{O}}}} \quad (5)$$

where TW and BW—quantities of TW and BW expressed per 100 g of ignited material; $\rho_{\text{H}_2\text{O}}$ —density of water; ρ_s —average density of acetone-dried CAC paste (including the hydrates and the fraction of nonreacted cement).

3. Results and discussion

Hardening of CAC pastes, mortars, and concrete is the result of the hydration process and can be studied indirectly through compressive strength and porosity measurements. The influence of different mass fraction of Li_2CO_3 on the compressive strength of CAC pastes has been studied, and the results of the measurement are given in the Tables 1–3 for water–cement (w/c) ratio 0.20, 0.25, and 0.30, respectively. The relation of strength and porosity is shown in Fig. 1. Shift of the data toward lower porosities for smaller w/c ratios used is observed. That is easily explained if initial porosities of the pastes prepared are calculated. At w/c ratio 0.20, 0.25, and 0.30 initial porosity of pastes prepared are 39%, 44%, and 49%, respectively ($BW=0$, $TW=100 \times w/c$, $\rho_{\text{CAC}}=3.20 \text{ g cm}^{-3}$). Thus, lower initial porosity of the material is responsible for the observed shift of the data. Total volume of cement paste expressed per 100 g of CAC corresponds to the denominator of the formula (Eq. (5)) and is shown in Table 4. Assuming that simple addition of volumes of CAC and water is valid, calculation shows that corresponding volumes of pastes containing 100 g of CAC at w/c ratios of 0.20, 0.25, and 0.30 are 51, 56, and 61 cm^3 , respectively, showing good agreement with experimental results (Table 4). Results of fitting previously mentioned models of compressive strength–porosity relation are given in Fig. 2 and in Table 5 for each w/c ratio investigated. Values of parameters σ_{P_0} in models of Hasselman, Balshin, and Ryshkewitch correspond to the compressive strength of nonporous material or equivalently to the extrapolated compressive strength of the CAC pastes to the zero porosity. The model of Schiller has a vertical asymptote at zero porosity, and the value of parameter

Table 3

Experimental results of compressive strength and porosity measurement for the CAC materials at $w/c=0.30$, prepared with the addition of Li_2CO_3

t (h)	σ (MPa)	TW (%)	BW (%)	ρ_s (g cm^{-3})	P (%)
$w(\text{Li}_2\text{CO}_3)=0\%$					
1	—	23.40	2.47	3.29	47.34
2	—	23.58	2.90	3.24	46.72
3	—	23.68	2.99	2.99	44.77
4	—	23.85	3.51	2.99	44.40
5	0.9	24.22	4.87	2.83	41.95
6	7.5	25.01	11.03	2.63	32.90
7	20.0	25.92	14.91	2.59	27.79
8	35.3	26.23	18.92	2.53	20.04
9	48.7	26.42	20.00	2.50	17.91
24	66.9	27.00	23.07	2.49	11.82
72	75.1	27.35	24.05	2.49	10.16
168	75.8	27.53	24.27	2.48	10.04
$w(\text{Li}_2\text{CO}_3)=0.001\%$					
1	—	23.65	4.38	3.12	44.05
2	—	23.99	5.62	3.00	42.03
3	0.5	24.31	7.70	2.89	38.81
4	2.3	25.07	14.41	2.48	26.08
5	7.8	26.10	15.96	2.53	25.77
6	11.3	26.28	18.03	2.47	21.66
24	47.3	26.31	20.67	2.33	15.13
72	57.5	27.04	22.59	2.29	12.26
168	68.6	27.36	25.42	2.27	5.72
$w(\text{Li}_2\text{CO}_3)=0.003\%$					
1	—	22.61	2.44	3.05	44.29
2	0.7	23.26	7.16	2.92	37.99
3	4.9	25.11	11.79	2.71	32.52
4	11.0	25.35	15.65	2.57	25.03
5	30.3	25.46	17.26	2.46	21.30
6	36.7	25.55	18.05	2.42	19.60
24	42.2	26.36	19.49	2.39	18.23
72	62.5	26.67	22.66	2.35	11.39
168	68.4	27.04	23.07	2.30	11.12
$w(\text{Li}_2\text{CO}_3)=0.005\%$					
1	0.2	22.85	4.92	3.16	42.34
2	3.1	23.54	8.03	2.98	37.68
3	21.2	24.54	14.33	2.82	27.62
4	32.2	24.79	16.91	2.75	22.37
5	35.0	24.91	17.42	2.69	21.16
6	40.0	25.02	18.62	2.60	18.16
24	46.7	25.16	19.35	2.48	16.14
72	48.8	25.72	20.40	2.66	16.00
168	65.9	25.88	23.19	2.49	8.29
$w(\text{Li}_2\text{CO}_3)=0.007\%$					
1	0.5	23.59	4.23	2.88	42.19
2	4.2	24.69	7.76	2.74	38.12
3	19.0	26.00	16.44	2.54	24.71
4	22.2	26.12	17.01	2.50	23.56
5	33.9	26.13	17.57	2.48	22.32
6	36.8	26.33	17.68	2.43	22.20
24	54.1	26.76	20.89	2.44	16.36
72	67.9	27.13	22.48	2.34	12.99
168	71.2	27.40	24.17	2.26	9.14
$w(\text{Li}_2\text{CO}_3)=0.010\%$					
1	1.2	23.06	4.50	3.00	41.98
2	7.8	23.51	10.64	2.91	32.87
3	31.7	23.58	15.63	2.70	21.93

Table 3 (continued)

t (h)	σ (MPa)	TW (%)	BW (%)	ρ_s (g cm^{-3})	P (%)
$w(\text{Li}_2\text{CO}_3)=0.010\%$					
4	38.7	24.03	17.65	2.57	17.75
5	51.9	24.03	18.34	2.52	15.88
6	58.6	24.20	19.02	2.51	14.64
24	69.7	24.38	19.89	2.51	12.97
72	70.1	25.02	20.89	2.39	11.63
168	79.8	25.95	23.12	2.33	8.18

k depends on the base of the logarithm so its value is merely a way of obtaining the best fit. The values of those parameters are approximately the same at all w/c ratios studied; thus, they were regarded as a constant for each model. Simple linear relationship of Hasselman shows artificial intercept with the abscissa at porosity less than the initial porosity and predicts negative strengths at higher porosities. Therefore, it is inadequate to represent strengths in the whole range of the porosity studied, which is in accordance with the assumptions used for its derivation [14] (Fig. 2). Models of Balshin and Ryshkewitch give almost identical values of the compressive strengths what is easily explained in terms of row expansion. High values of k are merely a way of obtaining the best fit and have no physical significance, thus leaving us with no perspective to predict its value. Even for freshly prepared CAC pastes, the calculated strengths are of the order of few MPa (Fig. 2). Although the initial porosity of the paste enters in the model of Schiller, the predicted strength increase with the decrease in porosity is too high and better fit is obtained if both k and P_0 are fitted freely. For the reasons stated above, we started with the development of a model of the compressive strength–porosity relation based on the simplified view of the hydration of CAC. The hydration is viewed as a process that effectively increases particle radius due to the precipitation of calcium–aluminum hydrates and connects cement particles, contributing to

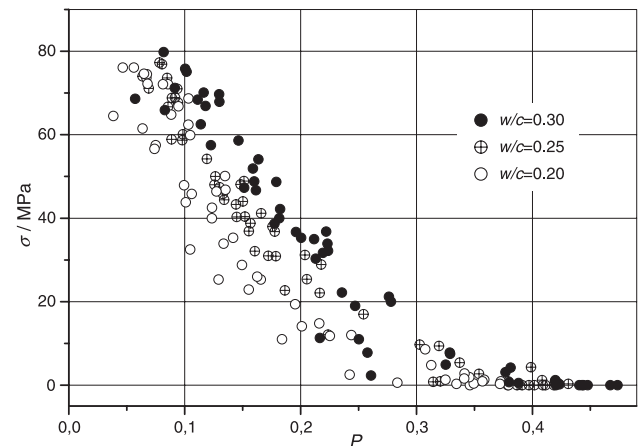


Fig. 1. Experimental data on strength–porosity dependence for CAC pastes prepared. Shift of the data toward lower porosities for smaller w/c ratios used is observed.

Table 4

Volume calculation of CAC paste according to Eq. (5), base is 100 g of CAC

w/c ratio	V_T/cm^3	V_E/cm^3
0.20	51.2	51.1 ± 2.9
0.25	56.2	55.5 ± 2.4
0.30	61.2	60.3 ± 4.5

V_T is the sum of the volume of CAC and water, and V_E is an average calculated from all the experimental data.

the increase in strength and decrease in porosity [9,15]. Taking different cross sections through the material, it is clear that the particular plane will intersect both solid material and empty or water-filled pores. If the cross section taken is big enough, then every plane will intersect, in the limit, fraction P of the porosity and $(1-P)$ of the solid material. Particularly, for fresh paste, the plane contains porosity, P_0 . At later ages, the advance of hydration increases the volume of solids, and porosity decreases. If we take into consideration the new contacts between particles, it is then reasonable to suppose that the grater is the number and density of interparticle contact, the greater is the strength. Regardless of the exact nature of the contact or the shape of the pores, as long as the decrease of porosity is random in space, it is possible to look at the intercept of the two different planes whatever their orientation. The intercept is a straight line that has probability of $(P_0 - P)/P_0$ times $(P_0 - P)/P_0$ that will contain newly formed interparticle contact. Thus, $\sigma \propto [(P_0 - P)/P_0]^2$, and the model between strength and porosity could be rewritten as (Eq. (6)):

$$\sigma = \sigma_{P_0} \left(1 - \frac{P}{P_0}\right)^2 \quad (6)$$

Constant σ_{P_0} contains microstructure factors involved, like density of CAC and calcium aluminate hydrates, particle size distribution and size, and density of flaws.

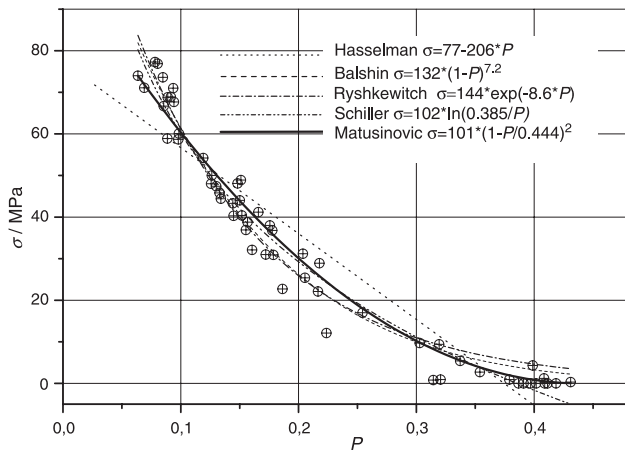


Fig. 2. Experimental data on strength–porosity dependence for CAC pastes at w/c = 0.25. Graphs of the best fit obtained for all the models tested are shown.

Table 5

Experimental data's obtained values for parameters σ_{P_0} , k , and P_0 for Hasselman, Balshin, Ryshkewitch, Schiller, and Matusinović models

Function	w/c = 0.20			w/c = 0.25			w/c = 0.30		
	k	σ_{P_0}	S.D. ²	k	σ_{P_0}	S.D. ²	k	σ_{P_0}	S.D. ²
$\sigma =$									
$\sigma_{P_0} - kP$	229	76	122	206	77	65	203	82	88
$\sigma_{P_0}(1 - P)^k$	8.2	122	63	7.2	132	15	5.7	123	63
$\sigma_{P_0}e^{-kP}$	9.7	135	70	8.6	144	20	6.9	134	78
$\sigma =$	P_0	k	S.D. ²	P_0	k	S.D. ²	P_0	k	S.D. ²
$k \ln(P_0/P)$	0.344 ^a	95	72	0.385 ^a	102	23	0.417 ^a	110	60
$\sigma =$	P_0	σ_{P_0}	S.D. ²	P_0	σ_{P_0}	S.D. ²	P_0	σ_{P_0}	S.D. ²
$\sigma_{P_0}(1 - P/P_0)^2$	0.390 ^b	96	63	0.444 ^b	101	23	0.490 ^b	106	48

S.D.² is estimate of the square of the standard deviation.

$$\text{S.D.}^2 = \frac{\sum_{i=1}^n (\sigma_{\text{experiment}} - \sigma_{\text{model}})^2}{n - n_{\text{parameters}}}$$

^a Better fit is obtained if both k and P_0 are regarded as parameters.

^b Calculated according to the Eq. (5).

Increase of strength of material is viewed as a consequence of the hydration process and decrease of porosity and size and density of flaws between any two points in the specimen under the complex stress state [16]. Results of fitting proposed functional dependence of compressive strength on porosity are given in Table 5. The matching of the proposed model fit is comparable or better than suggested previous models, although it contains only one adjustable parameter.

4. Conclusions

Compressive strength and porosity of CAC pastes and CAC pastes, prepared with the addition of lithium carbonate as a setting accelerator, had been studied at w/c ratios 0.20, 0.25, and 0.30. It was found that measurements of average density of acetone-dried CAC paste and quantities of TW and BW at different times of hydration are consistent. Functions relating strength and porosity proposed in the literature for various technical materials were tested on compressive strength–porosity data for CAC pastes. Most of the tested functions had shown good fit to our data, but parameter values are not easy to predict. Still, they also have unsatisfactory behavior at high porosity limit corresponding to the early ages of hydration. Model of compressive strength–porosity relationship proposed for CAC pastes is given by:

$$\sigma = \sigma_{P_0} \left(1 - \frac{P}{P_0}\right)^2$$

where σ represents the compressive strength, P porosity, P_0 porosity of fresh CAC paste, and the value of σ_{P_0} is an empirical constant. The advantage of the model is that it uses effectively only one empirical constant and that the

composition of material is accounted for. The model also describes well the high porosity range, starting from zero strength at initial porosity. Based on the generality of the assumptions used in the derivation of the model, we suppose that this model for CAC pastes can be applied for other cement materials as well as other similar materials.

Acknowledgements

The authors acknowledge the financial support from the Croatian Ministry of Science and Technology.

References

- [1] R. Salmoni, Verfahren zur Verkürzung der Abbindezeit von Tonerde-zementen, Deutsches Patent 648851, 1937 August.
- [2] A. Aldera, Fluidized Molding Material for Manufacturing Cores and Molds and a Method Therefore, U.S. Patent 3,600.203, 1969 September.
- [3] C. Hovasse, P. Allemend, Setting and Hardening of Aluminous Cement, U.S. Patent 3,826.665, 1974 July.
- [4] S.A. Rodger, D.D. Double, The chemistry of hydration of high alumina cements in the presence of accelerating and retarding admixtures, *Cem. Concr. Res.* 14 (1) (1984) 73–82.
- [5] J.H. Sharp, S.M. Bushnell-Watson, D.R. Payne, The effect of admixtures on the hydration of refractory calcium aluminate cements, in: R.J. Mangabhai (Ed.), *Calcium Aluminate Cements*, E & FN Spon, New York, 1990, pp. 127–141.
- [6] T. Matusinović, N. Vrbos, Alkali metal salts as set accelerators for high-alumina cement, *Cem. Concr. Res.* 23 (1) (1993) 177–186.
- [7] D. Damidot, A. Rettel, A. Capmas, Action of admixtures on fondu cement: Part 1. Lithium and sodium salts compared, *Adv. Cem. Res.* 8 (31) (1996) 111–119.
- [8] T. Matusinović, D. Čurlin, Lithium salts as set accelerators for high-alumina cement, *Cem. Concr. Res.* 23 (4) (1993) 885–895.
- [9] T. Matusinović, N. Vrbos, D. Čurlin, Lithium salts in rapid setting high-alumina cement materials, *Ind. Eng. Chem. Res.* 33 (11) (1994) 2795–2800.
- [10] M. Röbber, I. Odler, Investigations on the relationship between porosity, structure and strength of hydrated Portland cement pastes, *Cem. Concr. Res.* 15 (2) (1985) 320–330.
- [11] M.Y. Balshin, Dependence of mechanical properties of metal powders on porosity and limiting properties of metal–ceramic materials (in Russian), *Dokl. Akad. Nauk UzSSR* 67 (5) (1949) 831–834.
- [12] E. Ryshkewitch, Compression strength of porous sintered alumina and zirconia, *J. Am. Ceram. Soc.* 36 (2) (1953) 65–68.
- [13] K.K. Schiller, *Mechanical Properties of Non-Metallic Materials*, Butterworths Scientific Publications, London, 1959.
- [14] D.P.H. Hasselman, Relation between effects of porosity on strength and on young's modulus of elasticity of polycrystalline materials, *J. Am. Ceram. Soc.* 46 (11) (1963) 564–565.
- [15] S. Rashid, X. Turrillas, Hydration kinetics of CaAl_2O_4 using synchrotron energy-dispersive diffraction, *Thermochim. Acta* 302 (1) (1997) 25–34.
- [16] D.M. Roy, G.R. Gouda, Porosity–strength relation in cementitious materials with very high strengths, *J. Am. Ceram. Soc.* 56 (10) (1973) 549–550.